Lateral Diffusion of the Reconstituted Dialkyl Viologen Monolayer at the Air/Water Interface Studied with Electrochemistry

Don Keun Lee and Young Soo Kang*

Department of Chemistry, Pukyong National University, Daeyeon-3-dong, Nam-gu, Pusan 608-737, Korea

Received: July 3, 2003; In Final Form: January 30, 2004

The reconstituted dialkyl viologen monolayer at the air/water interface was studied as a model system of the biomembrane for the study of lateral diffusion of the electroactive viologen moiety because lateral diffusion of biomembrane molecules has key functions for the life phenomena. The shortest alkyl chain of 1,1′-didodecyl-4,4′-bipyridium dibromide ($C_{12}VC_{12}$) could not form the stable monolayer in the subphase of NaCl and NaBr aqueous solutions and also does not show any distinct phase transitions because it is partially soluble in the aqueous phase. For 1,1′-ditetradecyl-4,4′-bipyridium dibromide ($C_{14}VC_{14}$) and 1,1′-dihexadecyl-4,4′-bipyridium dibromide ($C_{16}VC_{16}$) molecules, the stable monolayer was obtained at the air/water interface, and this was identified with pressure−area isotherms and directly observed at Brewster angle microscopy (BAM) images. The changing orientation of alkyl chain of the viologenes was detected by surface potential measurements with moving barrier. Finally, the lateral diffusion of the viologen moiety of dialkyl viologenes at the air/water interface was successfully determined with electrochemical techniques using a microband electrode. The linear decrease of the diffusion constant of viologen molecules with decreasing mean molecular area and increasing alkyl chain length of viologenes at the air/water interface is explained by the decreasing free volume of the moving headgroup. This is well explained by the modified Cohen−Turnbull free volume model.

Introduction

The lateral motion of membrane components proves essential to the functioning of biomembrane systems. The specific molecular structure and composition of this lipid bilayer clearly demonstrate that forms and functions are inextricably intertwined. In such systems, any sort of chemical or physical perturbation may alter the membrane structure and its performance. Thermal agitation induces the movement of lipids and integral proteins in the plane of the lipid bilayer. This thermal movement in two dimensions is identical with lateral diffusion. Although a complete treatment must include both rotational and translational diffusion, for biological membranes, translational diffusion is by far the most important. A reorganization of the components to restore its original form can occur through lateral diffusion of the lipids.[1] Lateral diffusion of lipids in bilayer assemblies was first recognized and measured by Devaux and McConnel[l,2] and by Träuble and Sackmann[3] using ESR methods. Mobility of lipids has been a subject of considerable interest,[4−6] reflecting the importance of this class of quasi-two-dimensional assemblies and their dynamical properties as model systems of biological membranes.[7] Fluorescence spectroscopy has subsequently become a more popular and useful method in such lateral diffusion determinations.[8,9] Among the fluorescence techniques, fluorescence recovery after photobleaching (FRAP) has been proven to be fruitful in yielding accurate values of diffusion constants (D) for lipid molecules.[10,11] FRAP measures the regrowth of fluorescence due to the ability of probing molecules diffusing into a pulse photobleached region.[8] Peters and Beck made the most important contribution to the study of lateral diffusion in lipids on the water surface using FRAP.[9−11]

There is a new electrochemical approach that parallels FRAP in trying to understand lateral transport processes and the fluidity of membranes.[12] This is also to overcome the disadvantages of FRAP because FRAP has some limitations such as convection within the monolayer. This is minimized in the electrochemical technique using a microband electrode. However, the electrochemical method has limitations as well, most notably the need for an electrochemically active probe molecule. The electrochemical technique specifically examines the dynamics of lateral diffusion in Langmuir monolayers at the air/water interface. This technique has its early roots in studies that used electrochemical methods to study the diffusion of amphiphiles in bilayer assemblies.[12] Other concurrent studies also utilized electrochemistry in investigations of Langmuir monolayers, but they did not specifically probe lateral processes.[13] The key to the technique developed is a purposefully designed electrode that can address the monolayer assembly and lateral processes occurring within it. By use of this electrode, the dynamics of lateral transport can be examined because the measured peak current is directly proportional to the arrival rate of the molecules to the electrode surface.

Cyclic voltammetry is used to measure the lateral diffusion constant (D) for the amphiphiles in the monolayer structure. Voltammetric peak current can be used to calculate values of D for the system. The peak current was measured by extrapolating a straight line from the baseline and measuring its vertical distance in the cyclic voltammograms. Cyclic voltammograms obtained at the air/water interface during compressions provide a means of obtaining values of D while the surface concentration was changed. This was done using the following equation for the voltammetric peak current, i_p adapted for two dimensions:[14−16]

$$i_p = (2.69 \times 10^5)(n)^{3/2}(l)(D)^{1/2}(v)^{1/2}(\Gamma)$$

where n is the number of electrons involved, Γ is the surface concentration (mol/cm^2), D is the diffusion constant (cm^2/s), v

* To whom correspondence should be addressed. E-mail: yskang@pknu.ac.kr.

10.1021/jp0359236 CCC: $27.50
Published on Web 03/04/2004

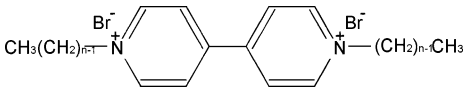

Figure 1. Structure of dialkyl viologenes (C_nVC_n, $n = 12$, 14, and 16).

is the scan rate (mV/s), and l is the electrode length (cm). In this model, two dimensions are equivalent to a linear potential sweep voltammetry of a reversible wave in a three-dimensional model.

The measurement of the surface potential has proved to be useful for characterizing the alkyl chain orientation of the molecules consisting of a monolayer at the air/water interface. The technique has provided valuable insight and quantitative information on a number of effects such as subphase pH and temperature, on the monolayer behavior and for identifying phase transitions resulting from molecular orientation during monolayer compression. There are three models for the dipole moment estimation from surface potential measurements of monolayers at the air/water interface.[18−20] In the previous studies, the surface potential of phospholipid, poly(L-lysine), stearic acid, and azobenzene monolayers at the air/water interface was studied in the same method.[21−24] The orientation of the alkyl chain of the molecule of the monolayer can be detected by the change of the surface potential of the monolayer at the air/water interface. The morphology and aggregation state change, phase transition, and Langmuir behavior of the monolayer were also studied with Brewster angle microscopy (BAM).[25−29] Although the organization of the organic molecules on the water surface may be inferred from these thermodynamic investigations, it was not until the advent of the imaging technique of BAM. This enabled us to examine the monolayer directly by observing images.

In the present study, The electroactive amphiphilic dialkyl viologens are used as a probe to investigate the lateral diffusion at the air/water interface because of the well characterized electrochemical properties and easy reconstitution to be a monolayer due to their insolubility into the aqueous phase. We focus on the dependence of the dialkyl viologen lateral diffusion coefficient at the air/water interface on its surface concentration, alkyl chain length, and the size of counterions.

The viologenes have been used as electroactive probe molecules on the monolayers of the solid substrate.[30−32] They also have been used as photoactive probes for the photoinduced charge separation studies by incoporating into the zeolites or molecular assemblies.[33−35] The homogeneity of the dialkyl viologen Langmuir monolayer was studied with pressure−area isotherms and BAM, and the lateral diffusion was studied with electrochemistry using a fabricated microband electrode. BAM images give the information on the stable monolayer formation, its phase transitions, and the collapse of the monolayer at a high surface pressure. The change of alkyl chain orientation of the monolayer of viologen molecules was studied by surface potential measurements.

Experimental Section

Materials. The electroacitve dialkyl viologen dibromides (C_nVC_n, $n = 12$, 14, and 16), of which structures are shown in Figure 1, were prepared by the procedures previously reported.[17] Organic solvents, such as chloroform and methanol, were either ACS certified spectroanalyzed or HPLC grade. All other chemicals, such as sodium chloride, sodium bromide, sodium iodide, and sodium perchlorate, were obtained from Aldrich Chemical Co. and used without any further purification. Stock solutions of 1 mg/mL dialkyl viologenes were prepared in a minimum amount of methanol and then diluted with chloroform to the desired concentration. House-distilled water was passed through a four-cartridge Barnstead Nanopure II purification train consisting of Macropure pretreatment, organic free, and a 0.2 μm hollow-fiber final filter for removing particles. Its resistivity was determined as 18.4 MΩ cm.

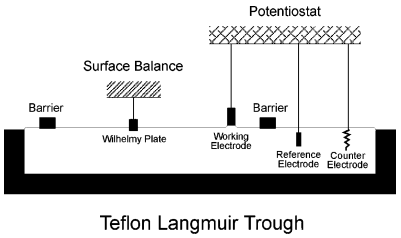

Figure 2. Experimental setup used in the electrochemical measurements of lateral processes in Langmuir monolayer.

Pressure−Area Isotherm and Electrochemical Experiments. The Langmuir trough for both isotherm and electrochemistry experiments (775 mm × 12 mm, KSV 2000 System 3) is housed within a large Plexiglas box to isolate it from the laboratory atmosphere, and setups are shown in Figure 2. The trough must be carefully placed to ensure that it was completely level and that there was a good seal between the trough and the barrier; this is essential to the monolayer compression. These jobs enabled us to keep the experiments from any significant noise for the surface pressure−area and surface potential−area isotherm and electrochemical measurements. After each experiment at the end of compression, the monolayer was carefully aspirated, and then the subphase was removed before the normal cleaning procedure was used. The setup includes a surface pressure microbalance that uses the Wilhelmy plate techniques. The KSV system was controlled by a PC-AT clone computer and DSV Dynamic Film Control System Software. Isotherm compression and data collection were achieved through the use of software. Cyclic voltammetry was performed with an Ensman model EI-400 bipotentiostat in a three-electrode configuration.

The reference electrode (SCE) and the Pt counter electrode were immersed in the subphase in a Langmuir trough behind the barrier as shown in Figure 2, where their presence did not interfere with a monolayer compression. The microband electrode was positioned at the air/water interface, following monolayer spreading and solvent evaporation. After the background current was recorded, the working electrode was lifted up, the monolayer was spread, and the microband electrode was carefully repositioned at the air/water interface. The working electrode was positioned at the air/water interface as shown in Figures 2 and 3 using a movable arm with an electrode clip. The monolayer-spreading solutions (1 mg/mL concentration) were prepared fresh daily by weighing and dissolving dialkyl viologenes in chloroform. To prepare a surface monolayer of surfactant, a 100 μL aliquot of a spreading solution was delivered in the different locations to the subphase surface with a Hamilton microliter syringe. The subphase temperature was controlled with a refrigerator circulator from Jeio-Tech Co. Ltd. (model RBC 20).

Surface Potential Measurements. The surface potential at the air/water interface was measured using the vibrating plate method (accuracy ±10 mV) of the surface potential-meter from KSV. The setups are shown in Figure 4. It assumes that a monolayer at the air/water interface may be divided into three layers, each making a distinct and unique contribution to the surface potential, ΔV.

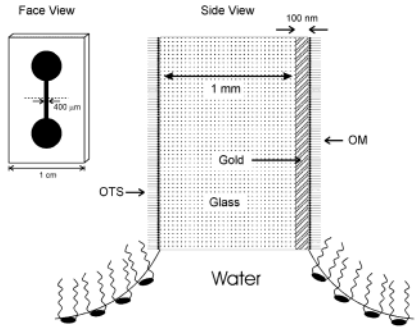

Figure 3. Microband electrode and its positioning at the air/water interface. A glass slide with the vapor-deposited gold film is marked by the shaded area. Water forms a positive meniscus by wetting the bottom edge of the glass slide. The one-dimensional electrode is the 100-μm-long line in the plane of the water surface, defined by the difference in wettability of the clean gold edge and of the octadecylmercaptan (OM)-coated gold surface above the water. The bottom edge of the glass slide in contact with water was created by snapping half of the electrode, which initially carried out a twin-pair electrode pattern. All gold and glass surfaces of the glass slide are nonwettable, since they are coated by a self-assembled monolayer of OM and octadecyltrichlorosilane (OTS), respectively.

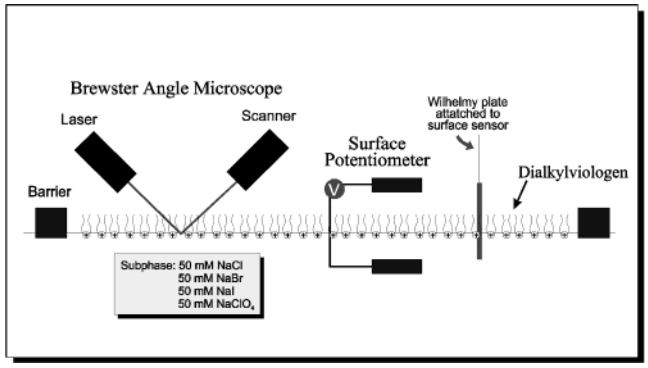

Figure 4. Experimental setups for the measurement of potential−area (V−A) isotherm and BAM image.

BAM Measurements. In the experimental setup of BAM (Nanofilm Tech., Germany) for the characterization of monolayer and interfacial processes, the light beam of a pulsed laser (λ = 532 nm, beam diameter 1 mm) passes a polarizer set for *p* polarization and is incident on the air/water interface at the Brewster angle (53.15°). The reflected beam was detected using a CCD camera. The interface to be studied is illuminated by a polarized parallel laser beam in the plane of incidence (*p*). The incidence angle is the Brewster angle that implies that no light is reflected if there is no interfacial layer and no roughness at the interface. The refractive index changes abruptly from the refractive index of one medium to that of the second medium at the level of the interface. Such changes depend strongly on the interfacial properties such as the molecular density and the orientation in the interfacial layer. In this way, an image of the interface can be formed through a microscope inclined at the Brewster angle, which collects the reflected light and a part of the light scattering by the interface.

Fabrication of the Micro-Band Electrode. The electrodes were produced by gold vacuum deposition on standard 3 × 1 in. glass microscope slides. To achieve the desired background characteristics of the microband electrodes, the usually 50−70 Å chromium underlayer was replaced by a surface film of (3-mercaptopropyl)trimethoxysilane, as described elsewhere, as a means of improving gold adhesion to the glass surface.[12] Metal masks were used to define the electrode pattern (see Figure 3). This consists of two circle contact pads of 0.2 cm in diameter and the line connecting them was 400 μm in width. This defines a twin pair of glass substrates along a line perpendicular to the gold strip approximately halfway between the contact pads. Typically, about 500−1000 Å gold (99.999%) films were deposited in a Veeco model 7700 bell jar operating at 2×10^{-7} Torr of base pressure. The next modification for the hydrophobicity of the electrode surface was carried out with a self-assembly of octadecylmercaptan (OM), which rendered the gold surface hydrophobic. The next and most critical step in the electrode fabrication was the self-assembly of octadecyltrichlorosilane (OTS) to create a hydrophobic monolayer on the glass surface. This electrode was then cut into sections containing individual twin electrode pairs. Individual electrode substrates were scribed on the back with a diamond pencil and fractured just before an electrochemical experiment.

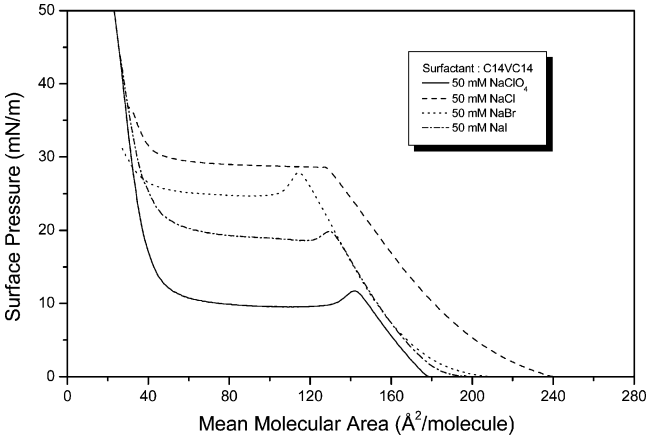

Figure 5. Pressure−area isotherms of ditetradecyl viologen in the subphase of the 50 mM of $NaClO_4$, NaCl, NaBr, and NaI at 25 °C.

Results and Discussion

Pressure−Area Isotherm. Figure 5 shows the pressure−area isotherms of ditetradecyl viologenes in the different subphases. The collapse pressure is reached at which the film irretrievably loses its mono-molecular form. It can be defined as the maximum to which a monolayer can be compressed without the detectable expulsion of molecules from the Langmuir film. The isotherm curves show that the collapse pressure of the monolayer of ditetradecyl viologenes increases with changing the subphase which includes counterions in 50 mM aqueous solution as $NaClO_4$ < NaI < NaBr < NaCl. This indicates that the stability of the monolayer is critically affected by the counterion of the subphase. In the first, this can be caused by the different size of counterions which are complexed with the positive moiety of viologene by the electrostatic interaction. The larger size of the ClO_4^- counterion can get the monolayer of ditetradecyl viologenes to be unstable because the positive charge of the viologen moiety of the monolayer can be easily wrinkled by the bulky counterion. On the other hand, the smaller counterion can be complexed more tightly than larger one, and this results in a more stable monolyer than that with larger counterions. Since kinds of counterions in the subphase, and therefore the extent of ion-pairing with Cl^-, Br^-, I^-, and ClO_4^- was altered,[13b] there should be some difference in the isotherms with four counterions. This in turn may affect the compressibility of the dialkyl viologen monolayers. In the second, the change in the size of counterion in the subphase may also affect the degree of the hydrodynamic coupling.[15,16] As shown in Figure 5, the isotherms are different in terms of shape and collapse pressure which, as mentioned prior, is a good indication of

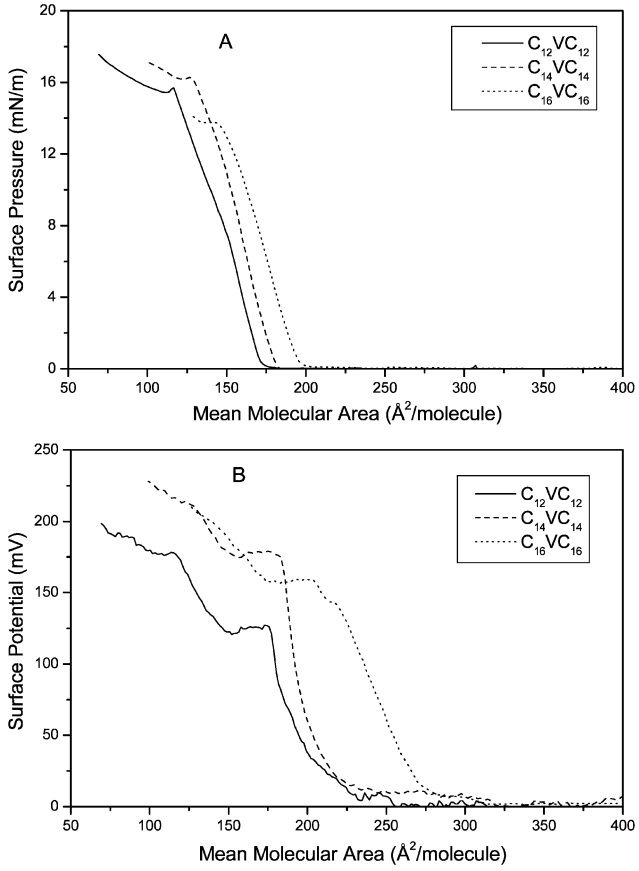

Figure 6. Pressure−area isotherms (A) and potential−area isotherms (B) of the three dialkyl viologenes with different alkyl chain length in the subphase of 50 mM NaI at 25 °C.

monolayer stability. The relative trend in collapse pressures antiparallels the trend in the size of counterions. The smaller size of counterion corresponds to a higher collapse pressure. Generally speaking, the size of counterions in the subphase affects the hydrophilic interactions with the subphase which, in turn, modifies its compressibility. These also affect not only the monolayer morphology but also its ability to diffuse at the air/water interface. Figure 6 shows pressure−area isotherms (A) and potential−area isotherms (B) of the three dialkyl viologenes with different alkyl chain length in the subphase of 50 mM NaI at 25 °C. The information on the formation of monolayer and alkyl chain orientation can be obtained from the combined work of the surface pressure−area isotherm and the surface potential−area isotherm. The surface potential of the monolayer at the air/water interface is concerned with the orientation and subphase composition.[18−20] The measurement of the surface potential has been proved to be useful for characterizing the alkyl chain orientation of the surfactant molecule of the monolayer at the air/water interface. The partial dipole compensation techniques was recently introduced by Vogel and Mobius.[21] The Demchak and Fort model[22−24] provides a good agreement between the group dipole moments of several aliphatic compounds estimated from the monolayer surface potential and the values determined for the same groups from measurements on bulk material. In view of success, the model of this study is based on the Demchak and Fort approach which itself was a refinement of the Helmholtz−Davies model and assumes that a monolayer at the air/water interface can be divided into three layers, each making a distinct and unique contribution to the surface potential. For the ionized monolayers, it is also necessary to include the double-layer potential. Thus, the surface potential can consist of the contribution from (a) the reorientation of water molecules in the subphase induced by the presence of the monolayer, (b) the group dipole moments associated with the hydrophilic headgroup region, and (c) the group dipole moments associated with the hydrophobic tail region of the monolayer. The headgroup charge and subphase composition is negligible because of almost the same factors in the experiment of C_{12}, C_{14}, and C_{16} dialkyl viologen. It is affected only by hydrophobic tails of dialkyl viologenes. Thus, the difference of the surface potential is due to the dipole moment change of hydrophobic alkyl chains of dialkyl viologenes, which results from the change of the orientation of the alkyl chains. As shown in Figure 6A, the didodecyl and ditetradecyl viologen molecules form more stable monolayer than C_{16} in the subphase of 50 mM NaI at 25 °C. The longer alkyl chain of alkyl viologenes results in the more oily monolayer films at the air/water interface even with complexation with the counterion in the subphase. This possibly results in the less stable monolayer. The surface potential is increased steeply around the takeoff point of the pressure−area isotherm curve (see Figure 6B). This suggests that the orientation of alkyl chains of dialkyl viologen molecules is greatly changed to perpendicular from the random direction around the takeoff point at the air/water interface. On the other hand, the earlier takeoff point of surface potentials of dihexadecyl viologen than didodecyl viologen or didecyl viologen can be interpreted as the longer alkyl chain of dihexadecyl viologen flips more easily from random orientation to perpendicular orientation to the air phase because of greater rigidity.

Brewster Angle Microscope (BAM). To observe the phase behavior and state of aggregation of three dialkyl viologen monolayers in the subphase of 50 mM NaCl, BAM images are taken in correlation with the mean molecular area of the monolayer of dialkyl viologenes at the air/water interface. The representative pressure−area isotherms were obtained with dihexadecyl viologen ($C_{16}VC_{16}$), ditetradecyl viologen ($C_{14}VC_{14}$), and didodecyl viologen ($C_{12}VC_{12}$) and are shown in the upper part of Figure 7. The more stable Langmuir monolayer was formed with $C_{16}VC_{16}$ and $C_{14}VC_{14}$. The less stable monolayer was formed with $C_{12}VC_{12}$ because of partial water solubility of the shorter alkyl chain of viologen. The longer alkyl chain of vologen results in an earlier takeoff point than that for shorter alkyl chain viologenes. This is due to the fact that the longer alkyl chain possibly allows a larger limiting area than the shorter one because of less headgroup immersion of the hydrophilic viologen moiety into the subphase. The greater degree entanglement of the alkyl chains of dialkyl viologenes by hydrophobic interaction possibly results in the movement of the headgroup position toward the air phase. This is a contrast to the previous results of isotherms with alkylferrocenecarboxamides and its mixed monolayer with phosphatidylcholine lipids.[15,16,44a] This is due to the difference of hydrophilicity between the positively charged viologen moiety and the neutral carboxamide headgroup because the less hydrophilic carboxamide headgroup cannot allow the movement of the headgroup by the increased alkyl chain length of molecules. This postulation will be discussed in the results of the electrochemical measurements in the following section.

The formation of a comparatively homogeneous phase of BAM images at a mean molecular area of 180 Å^2/molecule is shown in Figure 7, parts A and B. Unfortunately, there are partially aggregated regions of the viologen molecules. This was intrinsically detected at the room-temperature BAM images of violgenes because of the dimerization of molecules.[44b] So this

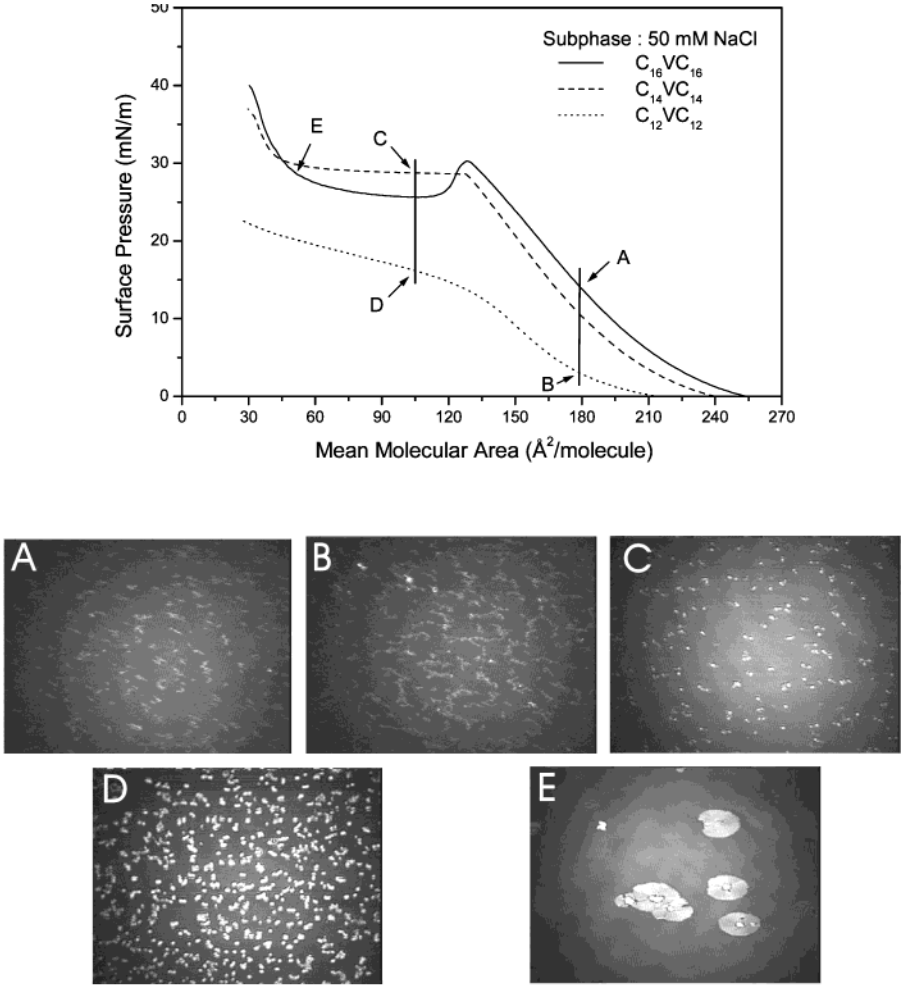

Figure 7. Pressure−area isotherms of the three dialkyl viologenes with different alkyl chain length (top) and BAM images (430 × 320 μm) of three dialkyl viologenes with different alkyl chain length at different mean molecular area of 180 Å^2/molecule (A and B), 105 Å^2/molecule (C and D), and 50 Å^2/molecule (E) in the subphase of 50 mM NaCl at 25 °C.

was suppressed as much as possible by decreasing the temperature of the subphase to 8−10 °C. This is also supported by the strangely larger limiting area of the monolayers of dialkyl viologenes compared with monoalkyl viologenes. The similar BAM images were obtained until the collapse region of the monolayer. As the barrier is compressed above the mean molecular area of 105 Å^2/molecule, the isolated domain images of BAM of dialkyl viologen molecules appeared by the partially aggregated molecules as shown in Figure 7, parts C and 7D. However, upon further compression above the collapse pressure, the growth of the solid aggregated domains of the dihexadecyl viologen monolayer molecule is clearly observed as shown in Figure 7E. The similar results are shown in other dialkyl viologene monolayers. This clearly shows the aggregation and growing mechanism of dialkyl viologen molecules. When the dialkyl viologen molecules begin to aggregate and grow to be bigger ones, the dynamics of the molecule possiblly suppressed more. This will be discussed in the following section.

Electrochemical Experiments at the Air/Water Interface. The representative cyclic voltammogram of the ditetradecyl viologen monolayer is shown in Figure 8. The shape of the voltammogram was what would be expected for a linear diffusion case. Lateral diffusion is the sole mechanism of charge transport observed in the dialkyl viologen Langmuir monolayer. The diffusion-controlled voltammograms are shown by the peak-to-peak separation as an averaged voltage of about 75−80 mV. This indicates that there can be some uncompensated resistance

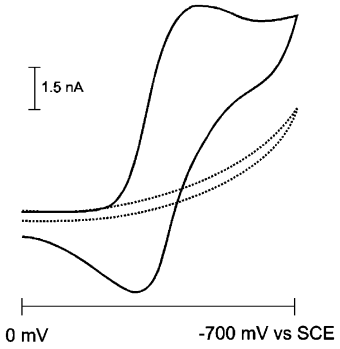

Figure 8. Representative cyclic voltammogram (—) of the ditetradecyl viologen monolayer in the subphase of 50 mM NaBr, with 200 mV/s of scan rate and 0−700 mV of scan range was recorded at the surface concentration (Γ) of 1.19 $\times 10^{-10}$ mol/cm^2 and background (- - -) was recorded on the same electrode before ditetradecyl viologen monolayer was spread on water surface.

in the system.[38] The peak separation may result from the quasi-reversibility of the viologen redox couple as well.

The linear increase of peak current with increasing $v^{1/2}$ as shown in Figure 9 indicates that the cyclic voltammogram of dialkyl viologen is a diffusion-controlled shape. The lateral diffusion of a dialkyl viologen monolayer at the air/water interface was studied by determining the peak current of the cyclic voltammogram. The lateral diffusion controls the charge transport along the Langmuir monolayer because charge trans-

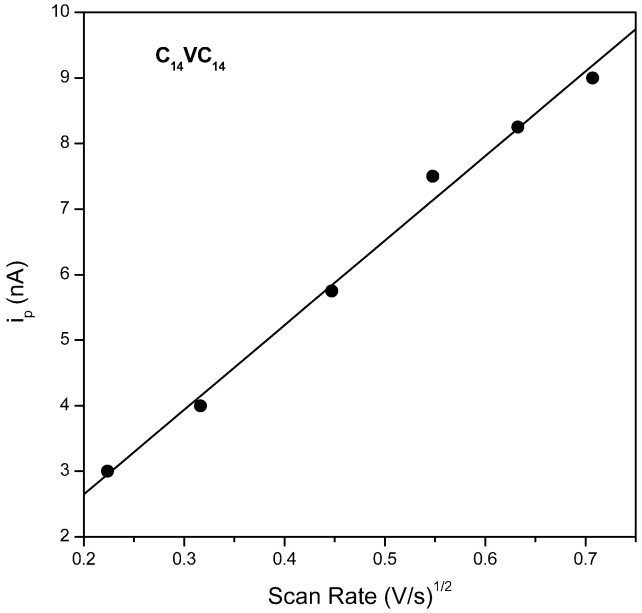

Figure 9. Peak current (nA) of ditetradecyl viologen monolayer in the subphase of 50 mM NaBr at 25 °C versus scan rate $(V/s)^{1/2}$ data at 200 Å^2/molecule.

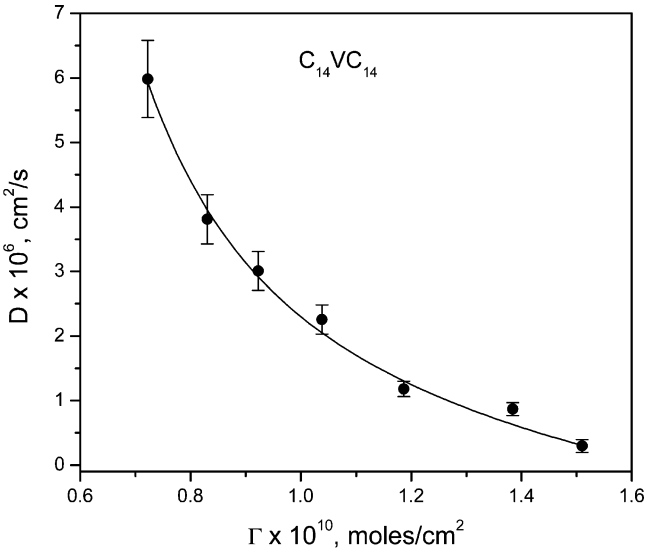

Figure 10. Plot of lateral diffusion constants of ditetradecyl viologen at the air/water interface versus ditetradecyl viologen surface concentration (Γ) in the subphase of 50 mM NaBr at 25 °C.

port can be controlled by two mechanisms such as lateral diffusion and electron hopping. Lateral diffusion is the sole mechanism of charge transport observed in the dialkyl viologen monolayers. This is due to the fact that the electron self-exchange rate constant of the oxidation−reduction couple systems of dicationic viologen to monocationic viologen ion is too small to compete kinetically with lateral diffusion.[45,46] The potential was scanned only over the first of the two viologen reduction waves so that the responses observed arise from the redox reaction at electrode.[47−49]

Figure 10 shows the plot of the ditetradecyl viologen lateral diffusion constant (*D*) at the air/water interface versus the ditetradecyl viologen surface concentration (Γ) in the subphase of 50 mM NaBr at 25 °C. The observed decrease of *D* versus surface concentration of the monolayer is an expected reflection of the decreasing fluidity of the monolayer assembly. For the experimental results shown in the plot of the diffusion constant (*D*) of the three different alkyl chain length of didodecyl,

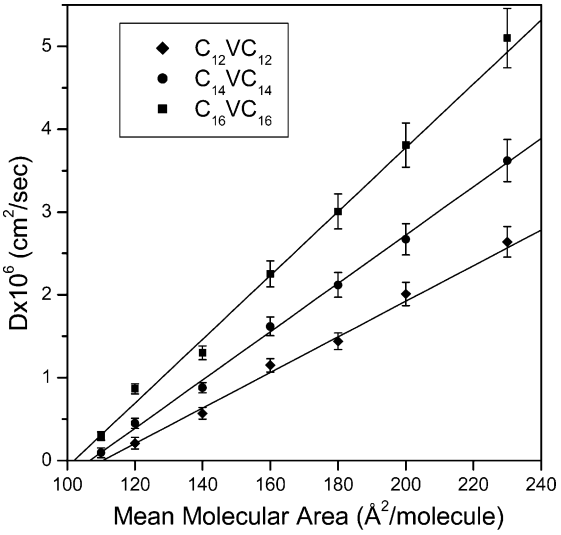

Figure 11. Plot of the diffusion constant (*D*) of the three different alkyl chain lengths (C_{12}, C_{14}, and C_{16}) of dialkyl viologenes versus the mean molecular area in the subphase of the 50 mM of NaBr, at 25 °C.

ditetradecyl, and dihexadecyl viologenes versus mean molecular area in the subphase of 50 mM of NaBr at 25 °C in Figure 11, each of the plots represents the average of three independent series of experiments with standard deviation shown by the error bars. As can be seen in Figure 11, there is a linear decrease of *D* with decreasing mean molecular area.

This can be explained by the Cohen−Turnbull free volume model, which considers the amphiphiles as a two-dimensional hard disk. Lateral diffusion is then analyzed as a random motion of a collection of disks limited only by the fluctuations in free area.[39] Qualitatively, this model states that the molecules move with gas-phase velocity whenever a fluctuation in density creates a void in their cage of residence. From the Cohen-Turnbull model, again adopted for the two-dimensional case, *D* is given by the following:[40]

$$D = gau \exp(-\gamma A^*/A_f)$$

where *g* is a geometric factor related to the dimensionality of the system, *a* and *u* are the mean displacement and gas-phase velocity of the molecule, *g* is a parameter with a value of 0.5−1.0 to correct for overlap of the free area, and A^* and A_f are the critical and free area per molecule.

The free area model has been used successfully to examine the concentration and temperature dependence of lipid diffusion measured by the FRAP technique. For example, Peters and Beck used the Cohen−Turnbull model to optimize the linearity of their plots by fitting the limiting mean molecular area of a lipid. It was shown earlier that when it is assumed that there is no minimum void area necessary and that the system behaves as a fluid at all free areas greater than zero the equation takes the following linear form:

$$D = gua\, A_f/\gamma$$

Since many of these parameters are unknown for our system, the model can only be applied in a qualitative manner to show that lateral diffusion is governed by the available free area. This leads to a linear increase of *D* with A_f. The model neglects all intermolecular interactions and explicitly ignores any hydrodynamic coupling of the amphiphiles to the subphase. These interactions must play a role in the diffusion of the dialkyl viologen monolayers at the air/water interface. The main

unprecedented finding in this study is that *D* increases with increasing chain length at any surface concentration of the viologen amphiphiles. These findings are diametrically opposed to what would be expected in view of molecular dynamics studies.[41,42] Calculations done in the previous study reported that the experimental value of *D* for a ferrocenecarboxamide was more than an order of magnitude smaller than expected by the molecular dynamic calculations.[15,37,44] The entanglement effect among the alkyl chains, which limited their lateral mobility, was proposed in the previous study.[37,44] In light of this, the diffusion of these monolayer molecules is supposed to be increased with decreasing chain length. The higher values of decreasing *D* with increasing alkyl chain length as shown in Figure 11 cannot be explained by the free area model alone. Clearly, a hydrodynamic coupling between the subphase and amphiphiles must be taken into account to give a more accurate explanation of the lateral diffusion. Specifically, the observed results can be explained by postulating that the extent of the dialkyl viologen monolayer coupling to the subphase was increased as its chain length was decreased. This is possibly explained by the fact that the position of the electroactive viologen moiety of shorter alkyl chain length with respect to the air/water interface shifts downward.

In other words, it appears that the diffusion of these molecules is affected not only by the lateral interactions covered by the free volume model but also by the viscous coupling of the amphiphiles' polar headgroup to the aqueous subphase. It is possible under the postulation that the extent of the viologen moiety coupling to the subphase was increased as its chain length was increased and that the position of the viologen moiety with respect to the air/water interface shifts downward. This suggests that the position of the molecule with respect to the interface is a result of a balance between the hydrophobic portion and hydrophilic interactions. In other words, both the energetics of the hydrophilic headgroup solvation as well as the van der Waals interactions between the alkyl chains have an effect on how the molecule is positioned.[42] The results also seem to indicate that the enthalpy of solvation becomes more negative as the molecule's position with respect to the interface is lowered. All of these pieces of information seem to be consistent with the recent molecular dynamic calculations of monolayers at the air/water interface, which show considerable water penetration into the headgroup region as well as an increase in the width of the water interfacial region when compared with a clean air/water interface.[43] The higher values of decreasing *D* with increasing alkyl chain length are possibly explained by the decreased hydrodynamic coupling of the hydrophilic electroactive viologen moiety to the subphase. This can be explained by the upward shifts of the viologen moiety due to the increased hydrophobic entanglement of longer alkyl chains. A plot of the diffusion constant (*D*) of ditetradecyl viologen versus mean molecular area in the different subphase of the 50 mM of $NaClO_4$, NaCl, NaBr, and NaI at 25 °C is shown in Figure 12. The decreasing lateral diffusion constant of ditetradecyl viologen with increasing size of counterions appears. This can be explained by the fact that the larger size of counterion suppresses the lateral mobility of the viologen headgroup due to the larger dynamic radius of the counterions. This can be explained clearly by the equation of Fick's first law on the diffusion coefficient.[49b] This is comparable to the ferroceneacrboxamide headgroup because of the positive headgroup charge of the viologen moiety of the dialkyl viologen molecules. The counterion with negative charge binds to the positive viologen headgroup and then decreases the lateral mobility of the hydrophilic viologen moiety

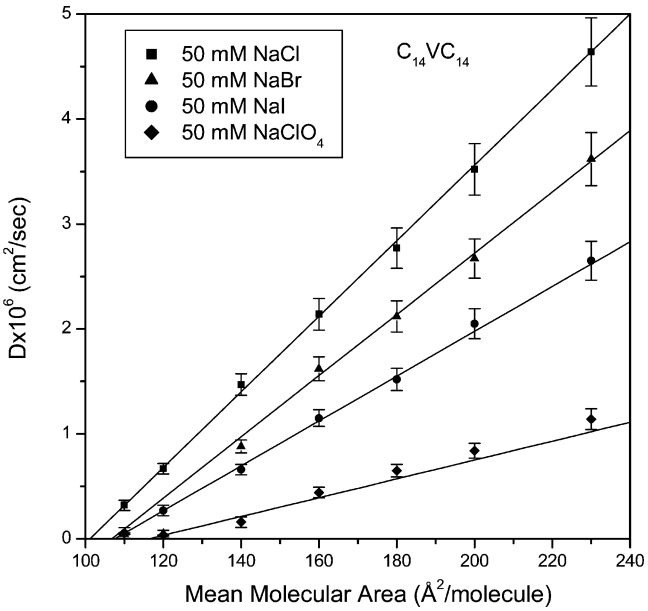

Figure 12. Plot of the diffusion constant (*D*) of ditetradecyl viologen versus mean molecular area in the different subphase of the 50 mM of $NaClO_4$, NaCl, NaBr, and NaI at 25 °C.

of the dialkyl viologen molecules. The degree of the lateral diffusion decrease became larger by the increased radius of the counterions of the monolayer. This interpretation is clearly shown by the decreasing lateral diffusivity of the tetradecyl viologen monolayer as NaCl > NaBr > NaI > $NaClO_4$. The lateral mobility decrease by the counterion effect of the neutral monolayers such as alkylferrocenecarboxamide did not so much appear by the different counterions.[50] It was interpreted that the negatively charged counterions do not bind so strongly by electrostatic interaction with the neutral ferrocene moiety to suppress the mobility of ferrocene headgroup even after oxidation of ferrocene. In the present study, the positively charged viologen moiety of the tetradecyl viologen monolayer is possibly suppressed by counterions in the decreasing order of NaCl > NaBr > NaI > $NaClO_4$ by the inverse order of counterion size. This indicates that the counterions suppress the lateral mobility of the monolayer headgroup by electrostatic interaction and the degree of lateral mobility decrease is critically affected by the counterion size. The observed *D* is an expected reflection of the decreasing fluidity of the monolayer.

Conclusively, dialkyl viologen molecules form the stable monolayers at the air/water interface, and this was investigated with pressure−area isotherms and Brewster angle microsscopy. The orientation change of the alkyl chain on viologen molecules was detected by surface potential measurements. Lateral diffusion of dialkyl viologen molecules at the air/water interface was successfully determined with electrochemical techniques using a micro-line electrode. The diffusion constant of viologen molecules at the air/water interface was decreased by decreasing the mean molecular area, decreasing the alkyl chain length of viologen molecules, and increasing the size of counterion in the subphase. These results show that the dialkyl viologen monolayer at the air/water interface can be used as a model system of biomembranes. This indicates that alkyl chain length and kinds of counterions can affect the lateral diffusion of monolayer.

Acknowledgment. This research is financially supported by Korea Science and Engineering Foundations (Project No. 971-0305-029-2).

References and Notes

(1) Edidin, M. In *Molecular Motions and Membrane Organization and Function*; North-Holland Biomedical Press: Amsterdam, 1981; Chapter 2.
(2) Devaux, P.; McConnel, H. M. *J. Am. Chem. Soc.* **1972**, *94*, 4475.
(3) Trauble, H.; Sackmann, E. *J. Am. Chem. Soc.* **1972**, *94*, 4499.
(4) Kim, S. H.; Yu, H. *J. Phys. Chem.* **1992**, *96*, 4034.
(5) Tamada, K.; Kim, S. H.; Yu, O. H. *Langmuir* **1993**, *9*, 3142.
(6) Tanaka, K.; Manning, P. A.; Lau, V. K.; Yu, H. *Langmuir* **1999**, *15*, 600.
(7) McConnell, H. M. *Annu. Rev. Phys. Chem.* **1991**, *42*, 171.
(8) Tessie, J.; Tocanne, J.; Baudra, A. *Eur. J. Biochem.* **1978**, *83*, 77.
(9) Peters, R.; Beck, K. *Proc. Natl. Acad. Sci. U.S.A.* **1983**, *80*, 7183.
(10) Cherry, R. J. *Biochim. Biophys. Acta* **1979**, *559*, 289.
(11) Peters, R. *Cell Biol. Int. Rep.* **1981**, *5*, 733.
(12) Miller, C. J. Ph.D. Thesis, University of California, Berkeley, California, 1987.
(13) (a) Zhang, X.; Bard, A. J. *J. Am. Chem. Soc.* **1989**, *111*, 8098. (b) Velazquez, C. S.; Hutchison, J. E.; Murry, R. W. *J. Am. Chem. Soc.* **1993**, *115*, 7896.
(14) Turnbull, D.; Cohen, M. H. *J. Chem. Phys.* **1970**, *52*, 3083.
(15) Kang, Y. S.; Majda, M. *Mol. Electron. Devices* **1995**, *6*, 25.
(16) (a) Kim, J. S.; Lee, S. B.; Kang, Y. S.; Park, S. M.; Majda, M.; Park, J. B. *J. Phys. Chem. B* **1998**, *102*, 5794. (b) (55) Kang, Y. S.; Majda, M. *J. Phys. Chem. B* **2000**, *104*, 2082.
(17) Pileni, M.-P.; Braun, A. M.; Gratzel, M. *Photochem. Photobiol.* **1980**, *31*, 423.
(18) David, M. T.; Osvaldo, N. O., Jr.; Hywel, M. *J. Colloid Interface Sci.* **1990**, *139*, 508.
(19) Osvaldo, N. O., Jr.; David, M. T.; Hywel, M. *Thin Solid Films* **1992**, *210*, 76.
(20) Arti, A.; Roberto, P.; Danilo, R.; Adriano, F. *Langmuir* **1997**, *13*, 5909.
(21) David, M. T.; Osvaldo, N. O., Jr.; Hywel, M *J. Colloid Interface Sci.* **1990**, *139*, 508.
(22) Osvaldo, N. O., Jr.; David, M. T.; Hywel, M. *Thin Solid Films* **1992**, *210*, 76.
(23) Arti, A.; Roberto, P.; Danilo, R.; Adriano, F. *Langmuir* **1997**, *13*, 5909.
(24) Cohen, S. M. A.; Wegh, R. A. J.; Kroon, J. M.; Suholter, J. R. *Langmuir* **1996**, *12*, 2863.
(25) Lheveder, C.; Henon, S.; Mercier, R.; Tissot, G.; Fournet, P.; Meunier, J. *Rev. Sci. Instrum.* **1998**, *69*, 1446.
(26) Cheng, Y.; Cunnane, V. J.; Kontturi, A. K.; Kontturi, K.; Schiffrin, D. J. *J. Phys. Chem.* **1996**, *100*, 15470.
(27) Oliveira, O. N., Jr.; Taylor, D. M.; Morgan, H. *Thin Solid Films* **1992**, *210*, 76.
(28) Maack, J.; Ahuja, R. C.; Tachibana, H. *J. Phys. Chem.* **1995**, *99*, 9210.
(29) Ahluwalia, A.; Piolanti, R.; De Rossi, D.; Fissi, A. *Langmuir* **1997**, *13*, 5909.
(30) Vidon, S.; Leblanc, R. M. *J. Phys. Chem. B* **1998**, *102*, 1279.
(31) Weidemann, G.; Brezesinski, G.; Vollhardt, D.; Mohwald, H. *J. Phys. Chem. B* **1998**, *102*, 1224.
(32) Tsao, M. W.; Fischer, T. M.; Knobler, C. M. *Langmuir* **1995**, *11*, 3184.
(33) Angelova, A.; Van der Aueraer, M.; Ionov, R.; Volhardt, D.; De Schryver, F. C. *Langmuir* **1995,** *11*, 3167.
(34) Hirano, K.; Fukuda, H. *Langmuir* **1995**, *11*, 4173.
(35) Oh, M. K.; Okajima, T.; Kitamura, F.; Lee, C. W.; Tokuda, K.; Ohsaka, T. *Chem. Lett.* **1997**, 67.
(36) Tam, K. Y.; Wang, R.; Lee, C. W.; Compton, R. G. *Electroanalysis* **1997**, *9*, 219.
(37) Park, Y. S.; Jang, J. M.; Lee, C. W. *J. Electroanal. Chem.* **1999**, *468*, 70.
(38) Yoon, K. B. Park, G. Y. *J. Am. Chem. Soc.* **1996**, *118*, 12710.
(39) Cohen, M. H.; Turnbull, D. *J. Chem. Phys.* **1959**, *31*, 1164−1169.
(40) Lee, D. K.; Kim, Y. I.; Kwon, Y. S.; Kang, Y. S.; Kevan, L. *J. Phys. Chem. B* **1997**, *101*, 5310.
(41) Angelova, A.; Volhardt, D.; Ionov, R. *J. Phys. Chem. B* **1996**, *100*, 10710.
(42) Pileni, M.-P.; Braun, A. M.; Gratzel, M. *Photochem. Photobiol.* **1980**, *31*, 423.
(43) David, M. T.; Osvaldo, N. O. Jr.; Hywel, M. *J. Coiloid Interface Sci.* **1990**, *139*, 508.
(44) (a) Osvaldo, N. O., Jr.; David, M. T.; Hywel, M. *Thin Solid Films* **1992**, *210*, 76. (b) Fernandez, A. J.; Martin, M. T.; Ruiz, J. J.; Munoz, E.; Camacho, L. *J. Phys. Chem. B* **1998**, *102*, 6799.
(45) Arti, A.; Roberto, P.; Danilo, R.; Adriano, F. *Langmuir* **1997**, *13*, 5909.
(46) Cohen Stuart, M. A.; Wegh, R. A. J.; Kroon, J. M.; Sudholter, J. R. *Langmuir* **1996**, *12*, 2863.
(47) Bird, C. L.; Kuhn, A. T. *Chem. Soc. Rev.* **1981**, *10*, 49.
(48) Kim, J. S.; Lee, S. B.; Kang, Y. S.; Park, S. M.; Majda, M.; Park, J. B. *J. Phys. Chem. B* **1998**, *102*, 5794.
(49) (a) Bard, A. J.; Faulkner, L. R. *Electrochemical Methods*; John Wiley & Sons: New York, 1980. (b) Silbey, R.; Alberty, R. A. *Physical Chemistry*; John Wiley & Sons: New York, 2001.
(50) Charych, D. H.; Landau, E. M.; Majda, M. *J. Am. Chem. Soc.* **1991**, *113*, 3340.